NJC

Accepted Manuscript

This is an *Accepted Manuscript*, which has been through the Royal Society of Chemistry peer review process and has been accepted for publication.

Accepted Manuscripts are published online shortly after acceptance, before technical editing, formatting and proof reading. Using this free service, authors can make their results available to the community, in citable form, before we publish the edited article. We will replace this *Accepted Manuscript* with the edited and formatted *Advance Article* as soon as it is available.

You can find more information about *Accepted Manuscripts* in the Information for Authors.

Please note that technical editing may introduce minor changes to the text and/or graphics, which may alter content. The journal's standard Terms & Conditions and the Ethical guidelines still apply. In no event shall the Royal Society of Chemistry be held responsible for any errors or omissions in this *Accepted Manuscript* or any consequences arising from the use of any information it contains.

ROYAL SOCIETY OF CHEMISTRY

www.rsc.org/njc

Nanocomposites with both structural and porous hierarchy synthesized from Pickering emulsions – Towards conductive capsules

Carlos Avendano,[1] Nicolas Brun,[*,1] Eléonore Mourad,[1] Olivier Fontaine,[1,3] Christine Labrugère Sarroste,[4] Mohamed Baccour,[1] Martin In,[2] Ahmad Mehdi,[1] Antonio Stocco[2] and André Vioux[*,1]

[1]Institut Charles Gerhardt de Montpellier, UMR 5253, CNRS-ENSCM-UM, Université de Montpellier, CC 1701, Place Eugène Bataillon, 34095 Montpellier, France

[2]Laboratoire Charles Coulomb, UMR 5221, CNRS-UM, Université de Montpellier, CC069, Place Eugène Bataillon, 34095 Montpellier, France

[3]Réseau sur le Stockage Electrochimique de l'énergie (RS2E), FR CNRS

[4]PLACAMAT UMS3626, CNRS-Université de Bordeaux, 87 av. docteur Albert Schweitzer, 33608 Pessac Cédex France

Abstract

Commercial carboxymethylcellulose was used to prepare dispersible multi-walled carbon nanotubes-based composites. These composites were employed to prepare Pickering oil-in-water emulsions. Emulsion-templated macroporous materials were then prepared by embedding the oil droplets into a polymer resin arising from the polycondensation of furfural and phloroglucinol within the continuous aqueous phase in the presence of $FeCl_3$ as catalyst. Polymerization afforded organic-inorganic nanocomposite materials in the form of capsules. After pyrolysis, highly microporous, magnetic and electrically conductive micrometric capsules could be obtained. This approach opens interesting prospects for catalysis, separation and electrochemistry applications.

Introduction

Materials with structural and porous hierarchy, which provides outstanding accessibility to the internal surface, are of particular interest for advanced applications ranging from heterogeneous catalysis, separation, sorption as well as energy storage and conversion.[1] Drawing their inspiration from nature, chemists and physical chemists have been developing and combining various synthetic strategies, involving sacrificial templates, long-range weak interaction forces and/or self-assemblies, to prepare materials with structural and porous hierarchy.[2-6] In this study, we propose to take advantage of both the outstanding mechanical properties of carbon nanotubes to build resistant highly open architectures and their ability to stabilize oil-in-water Pickering emulsions, which makes it possible to template macroporous polymer nanocomposites.

As compared with classical emulsions, using molecular surfactants to stabilize liquid-liquid interfaces, Pickering emulsions are stabilized by solid particles.[7-9] The strong, if not irreversible, adsorption of solid particles at liquid-liquid interfaces makes Pickering emulsions highly stable against coalescence. Thus, such emulsions have been widely employed for the templating of macroporous materials.[10-16] Depending on several parameters – such as the nature of particles and the volume fraction of the dispersed phase – direct (oil-in-water), reverse (water-in-oil), diluted and/or concentrated emulsions could be formulated, leading to the generation of either discrete capsules[15, 16] or cellular foams[11].

Among particles used to stabilize emulsions, carbon nanotubes (CNTs) and graphenes are particularly interesting as they exhibit singular physico-chemical properties. Whatever the kind of emulsions used (direct or reverse), the adsorption of carbon particles at oil/water interface requires pre-treatments to make them amphiphilic. Thus, graphene oxide (GO)[17] and oxidized carbon nanotubes[18, 19] have been shown to stabilize liquid-liquid interfaces. Recently, Raston *et al.*[17] obtained hollow spheres from toluene-in-water emulsions stabilized by graphene oxide (GO). In the same vain, Shi *et al.*[20] could prepare highly compressible and electrically conductive macroporous monoliths from GO-based Pickering emulsions. A hydrothermal process was used to convert GO sheets to conductive reduced-GO. As for CNTs, plasma or acid treatments are typically used to make them partially hydrophilic.[21] However, such harsh treatments lead to some degradation of their electronic structure, to the detriment of their singular physico-chemical properties. Another strategy is to use polymers or

biopolymers[22] – such as cellulose[23], carboxymethylcellulose[24, 25] or amylose[26] – to functionalize and disperse carbon nanotubes in water.

In the present work, we chose to use commercial carboxymethylcellulose (CMC) to prepare dispersible multi-walled carbon nanotubes-based composites. These composites were employed to prepare Pickering oil-in-water emulsions Further polycondensation confined within the continuous aqueous phase of such emulsions allowed obtaining organic-inorganic nanocomposite materials in the form of capsules.

Experimental

Chemicals

Multi-walled Carbon Nanotubes (MWCNTs) (6-9 nm in diameter and ~5 µm in length with purity over 95%), sodium carboxymethylcellulose salt (NaCMC), anhydrous cyclohexane, furfural (>98%), phloroglucinol (>99%) and iron chloride hexahydrate (>97%) were purchased from Sigma-Aldrich and used as received. Sodium hydroxide anhydrous pellets were purchased from Carlo Erba Reagents. All chemicals were used as received without any purification or modification.

Preparation of Pickering emulsions stabilized by MWCNT-CMC composites

Typically, dispersions using sodium carboxymethylcellulose (NaCMC) were achieved mixing 100 mg MWCNTs and 100 mg NaCMC in a 500 mL aqueous solution at pH 7. The above mixture was ultrasonicated at 21 % amplitude using a 13 mm probe for 15 min. The sample was then centrifuged at 10,000 rpm for 10 min. The supernatant liquid was separated, concentrated by means of a rotary evaporator, then dried; this dispersible fraction was thereafter called **MWCNT-CMC**.

A small amount (10 mg) of the as-obtained **MWCNT-CMC** composite was re-dispersed in 10 mL of water at pH 7, sonicated with the dipping ultrasonic probe for 15 minutes. After cooling to room temperature, stable **MWCNT-CMC** dispersions with a composite concentration of 0.10 wt % were obtained.

Pickering emulsions were prepared as described above. Cyclohexane (3 mL) was added to a 10 mL **MWCNT-CMC** aqueous dispersion, and shaken by hand for 30 sec. The premix was emulsified by ultra-turrax disperser at 16,200 rpm for 3 min, then twice at 20,000

rpm for 1 min (IKA, T 18 digital). The emulsions were shaken by hand for 30 sec before each ultra-turrax treatment.

Emulsion-templated polycondensation of phloroglucinol with furfural

Typically, phloroglucinol (125 mg; 1 mmol) and furfural (163 µL; 2 mmol) were mixed in 600 µL water and 200 µL ethanol, and then subjected to an ultrasound bath for 5 minutes (**solution A**). Additionally, a Lewis-acid catalyst, *i.e.* Iron (III) chloride hexahydrate (54 mg; 0.2 mmol), was dissolved in 400 µL water (**solution B**).

Typically, 400 µL from brown **solution A** and 200 µL from yellow **solution B** were added to a 15 mL screw cap vial (SUPELCO) containing 5 mL Pickering emulsion. The vial was agitated by hand over a few seconds. Then, the mixture turned black and became highly viscous. The as-obtained gel, named **MWCNT-CMC-p**, was aged overnight at 60°C in a closed vial and dried at 80°C for 4 days in an open vial. To prepare conductive carbonaceous materials, the dried gel was placed in a quartz tube within a carbonization tubular furnace and heated up to 550 or 900 °C for 4 h under an inert atmosphere (*i.e.*, argon; flow: 10 $mLmin^{-1}$). A ramp was used to reach the desired temperature at a speed of 5 °C per minute. The samples were named **MWCNT-CMC-p-550** and **MWCNT-CMC-p-900**, respectively.

Characterisation

Pickering emulsions were observed by optical microscopy with a Leitz Laborlux 12 Pol S and images were processed using the program MGrabSequence. Scanning electron microscopy (SEM) was carried out using a Hitachi S4800. For transmission electron microscopy (TEM), an aliquot of sample was dropped on a holed carbon microscopy grid and micrographs were obtained using a JEOL 2200FS operating at 200 keV. A ThermoFisher Scientific K-ALPHA spectrometer was used for surface analysis with a monochromatized AlKα source (hν=1486.6eV) and a 200 microns spot size. A pressure of 3.10^{-7} Pa was reached in the chamber when transferring the powders pressed onto Cu tape. The full spectra (0-1350 eV) were obtained with a constant pass energy of 200eV and high resolution spectra (C1s, O1s, Fe2p,…) at a constant pass energy of 40eV. Charge neutralization was applied during analysis. Sputtering was performed with Ar^+ ions at 500eV low mode. High resolution spectra were fitted and quantified using the AVANTAGE software provided by ThermoFisher Scientific (Scofield sensitivity factors used for quantification). X-ray diffraction patterns were recorded on a Burker D8 Advance diffractometer and CuKα radiation (λ = 0.15406 nm) as

incident beam. Electrical conductivity measurements were performed on a VSP-300 Bio-Logic potentiostat. Conductivity was measured by electrochemical impedance spectroscopy with a range frequency from 5 to 1 MHz for **MWCNT-CMC-p-550** and **MWCNT-CMC-p-900** powdered samples; and from 5 MHz to 5 mHz for the MWCNT-CMC native composite. N_2 sorption analyses were performed at 77 K using a Micromeritics Tristar 3000, equipped with automated surface area and pore size analyzer. Before analysis, samples were degassed at 250 °C for 7 h using a Micromeritics VacPrep 061 degasser. BET surface areas were determined in the relative pressure range P/P_0 from 0.01 to 0.03.

Results and discussion

In a previous work, MWCNTs-Sigmacell cellulose composites could be dispersed in water at pH 10.5 and used to stabilize Pickering oil-in-water emulsions.[27] These emulsions tolerated pH modifications over a wide range, without significant change of droplets diameters. In particular, while decreasing pH from 10.5 to 6.8, creaming could be observed with the appearance of two distinct layers. This behavior could be explained by the poor dispersibility of MWCNTs-Sigmacell cellulose composites at pH lower than 10.5.[27]-Herein, we show that our approach can be extended to another polysaccharide, carboxymethylcellulose (CMC). Dispersible and conductive MWCNTs-CMC composites could be prepared (Figure 1 and ESI). As compared with Sigmacell cellulose, CMC allowed obtaining stable MWCNTs dispersions over a wider range of pH, from pH 7 to 10.5 (see ESI). Interestingly, as compared with Sigmacell,[27] Pickering emulsions could be directly obtained at pH 7 (Figure 2a) without creaming.

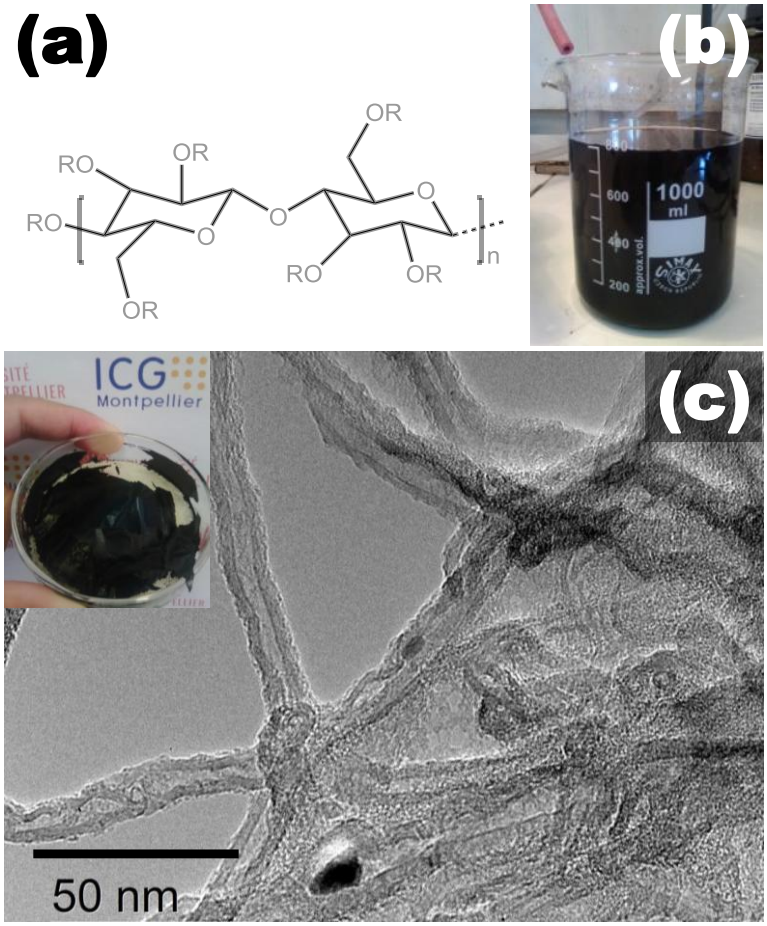

Figure 1. (a) Chemical structure of carboxymethylcellulose sodium salt (NaCMC). R = H or $CH_2CO_2^-$ Na^+. (b) Picture of a MWCNT-CMC dispersion in water at pH 7. (c) Picture (inset) and TEM micrograph of MWCNT-CMC composite used in this work.

Herein, we went one step further, employing emulsions stabilized by MWCNT-CMC at pH 7 for the design of functional conductive materials. Diluted Pickering emulsions were formulated as described in the experimental section, setting a cyclohexane volume fraction of 0.23. Emulsion-templated porous materials were then prepared by embedding the oil droplets into a polymer resin. Accordingly, the polycondensation of furfural and phloroglucinol was implemented within the continuous aqueous phase in the presence of a Lewis acid catalyst (Figure 3), iron chloride, as reported earlier for classical emulsions.[28] After polycondensation, aging and drying, emulsion-templated materials with typical morphologies were obtained as shown by scanning electron microscopy (SEM; Figure 2b-c). Such morphologies, made of aggregated hollow spheres, suggest that polycondensation started at the interfaces. To explain this feature, it is assumed that oil/water interfaces can be seen as defects where the enthalpy of nucleation is lowered.[29] Also, in our study, the density of MWCNT-CMC composites is most

probably higher at the interface, providing some more defects and anchoring points where polycondensation could preferentially start. Chemical reactions with hydroxyl and carboxymethyl groups of carboxymethylcellulose cannot be excluded.

At first sight, **MWCNT-CMC-p** looked like a fragile monolith made of aggregated capsules as shown in Figure 2b. However, after handling, aggregates together with discrete capsules could be obtained. Some protuberances (Figure 2c), could be observed, due either to flocculation phenomena or to heterogeneous nucleation of furfural-phloroglucinol particles during polycondensation.

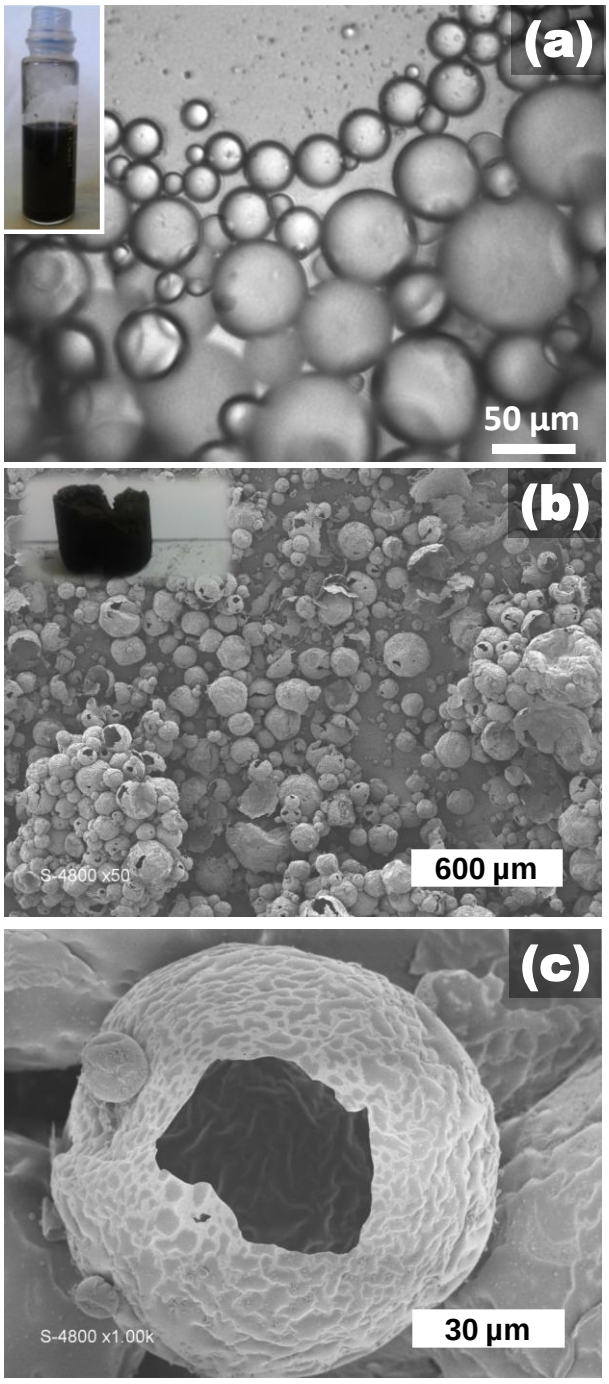

Figure 2. (a) Optical image and picture (insert) of the starting oil-in-water emulsion. (b-c) Scanning electron micrographs and picture (insert) of the as-obtained capsules **MWCNT-CMC**-p after polycondensation.

While MWCNT-CMC composites were initially conductive (see ESI for electrochemical impedance spectroscopy data, Table S1, and scanning electrochemical microscopy, Figure S1), **MWCNT-CMC-p** capsules obtained after polycondensation of furfural-phloroglucinol precursors exhibited high electrical resistivity. In order to recover

electron conduction, further thermal treatments were performed under inert atmosphere, *i.e.* argon. Whatever the temperature used, 550 or 900 °C, capsules were preserved as showed SEM micrographs (Figures 4a-b). Interestingly, as-prepared **MWCNT-CMC-p-550** and **MWCNT-CMC-p-900** both displayed magnetic behavior (Figure 4a; inset). This point will be discussed later. At higher magnification, surface roughness and heterogeneities were revealed (Figures 4c-f). While some dense protuberances were still present (Figures 4d-f), some "nude" domains resembled lace-like structures, most probably made of carbon nanotubes-based airy assemblies (Figure 4c).

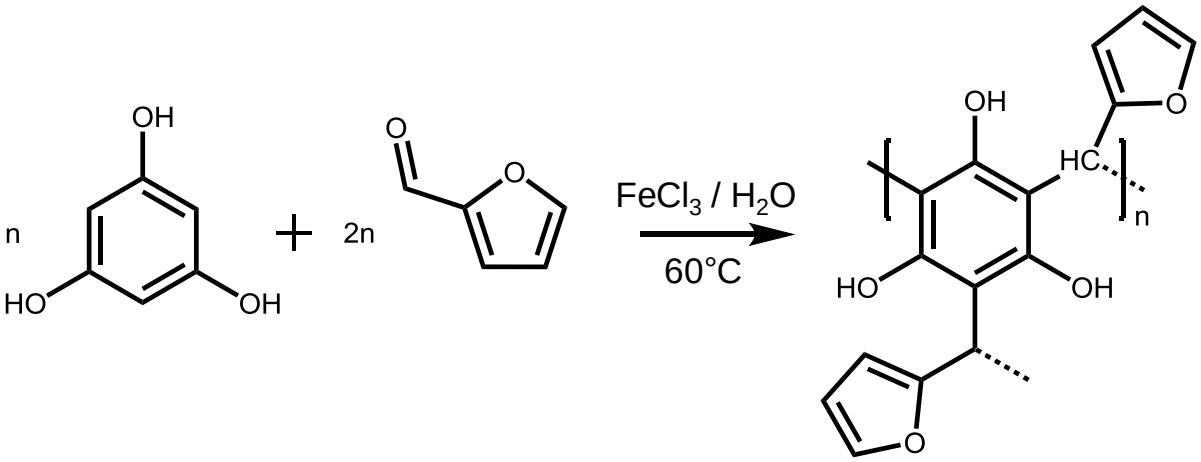

Figure 3. Polycondensation of phloroglucinol with furfural catalyzed by iron chloride at 60°C in water and probable structure of the as-obtained crosslinked resin. Adapted from Saad et al.[30]

This feature suggests that polycondensation was not homogeneous on the overall liquid-liquid interface, maybe due to close contacts between some droplets and lack of accessibility. Apart from protuberances, SEM micrographs showed thin shells of few hundred nanometers in which carbon nanotubes seemed embedded in dense coatings (Figure 4f). Transmission electron microscopy (TEM) allowed us to observe closely both "nude" and thin domains of the shells (Figure 5). Figure 5a showed a tangle of carbon nanotubes observed for **MWCNT-CMC-p**. As compared with MWCNT-CMC composites used initially (Figure 1c), the tubes look thicker, about 20 nm instead of 10 nm. Obviously, polycondensation occurred on MWCNT-CMC assemblies, leading to higher external diameters. After further thermal treatment at 900 °C, spherical particles with diameter of about 10 nm could be also observed apart from carbon nanotubes (Figures 5b-c). Considering the weak contrast at the interfaces between nanoparticles and the matrix, TEM micrographs suggest embedded particles in amorphous coatings rather than surface nucleation.

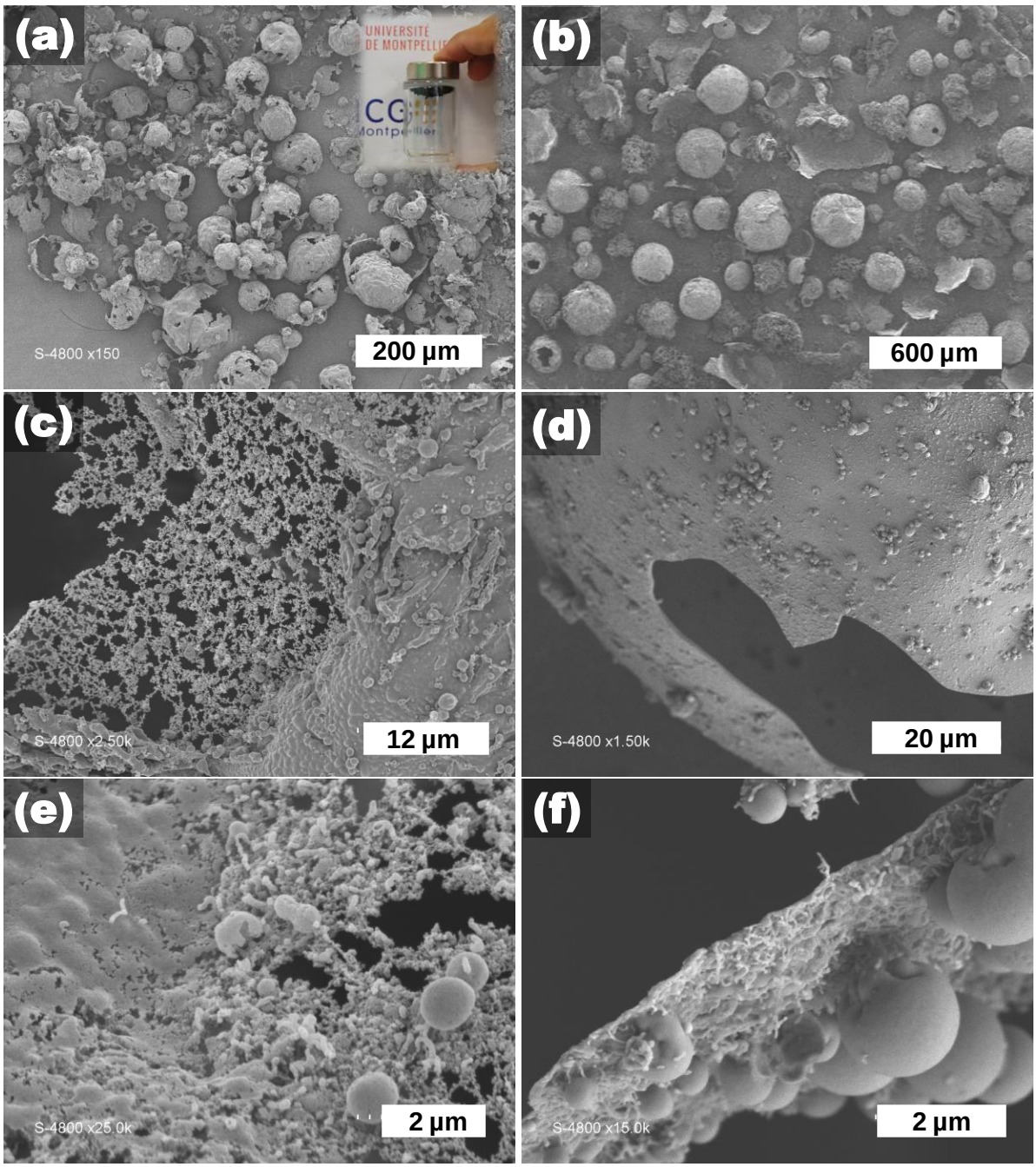

Figure 4. Scanning electron micrographs of **MWCNT-CMC-p** after further thermal treatment at (a-c-e) 550 °C (**MWCNT-CMC-p-550**) and (b-d-f) 900 °C (**MWCNT-CMC-p-900**) under argon. Inset in (a): picture of carbonaceous capsules attracted by a magnet.

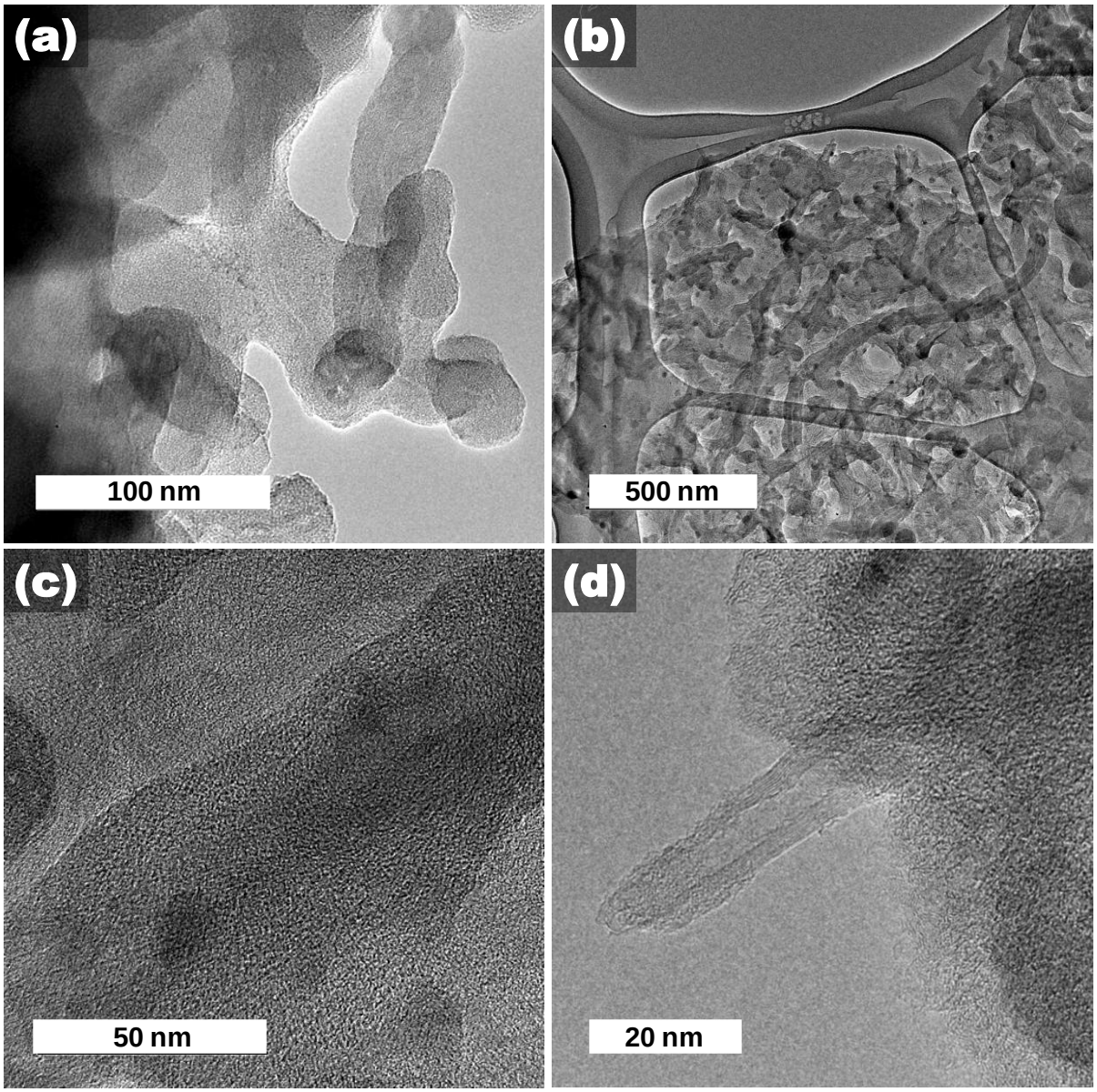

Figure 5. Transmission electron micrographs of **MWCNT-CMC-p** (a) before and (b-d) after further thermal treatment at 900 °C under argon.

In order to determine the structure and the chemical composition of these nanoparticles, X-ray diffraction (XRD; Figure 6) and X-ray photoelectron spectroscopy (XPS; Figure 7 and Table 2) were carried out. XRD patterns recorded for both **MWCNT-CMC-p-550** (Figure 6b) and **MWCNT-CMC-p-900** (Figure 6c) matched the standard XRD pattern of the spinel structure of both magnetite Fe_3O_4 (JCPDS card no. 85-1436) and maghemite γ-Fe_2O_3 (JCPDS card no. 04-0755) crystalline phases.[31, 32] Main peaks at 30°, 35°, 43°, 57° and

62.5° could be attributed to (220), (311), (400), (511) and (440) diffraction peaks, respectively.[31] The formation of iron oxide particles within the carbonaceous framework clearly explains the magnetic behavior observed earlier (Figure 4a; inset). Apart from the one at 43°, which could be also attributed to graphitic (100/101) lines originating from MWCNTs, diffraction peaks related to magnetite were not observed for MWCNT-CMC-p (Figure 6a). Thus, before further thermal treatment, iron element was most probably still as a salt and not as an oxide yet.

Interestingly, the main diffraction peak initially observed for pristine MWCNTs, *i.e.* graphitic (002) lines centered at 25.6° (see ESI), vanished. One question arises: were carbon nanotubes affected by furfural-phloroglucinol polycondensation? As TEM micrographs revealed flawless nanotubes after further thermal treatment at 900 °C (Figure 5d), one may assume that the absence of distinctive diffraction peaks may be due to a low loading of MWCNTs within the amorphous framework. Another interesting feature is related to the absence of graphitic (002) lines after further thermal treatment at 550 and 900 °C, suggesting a poor graphitization of the carbonaceous framework, despite efficient carbonization (decrease of O/C ratio; Table 2).

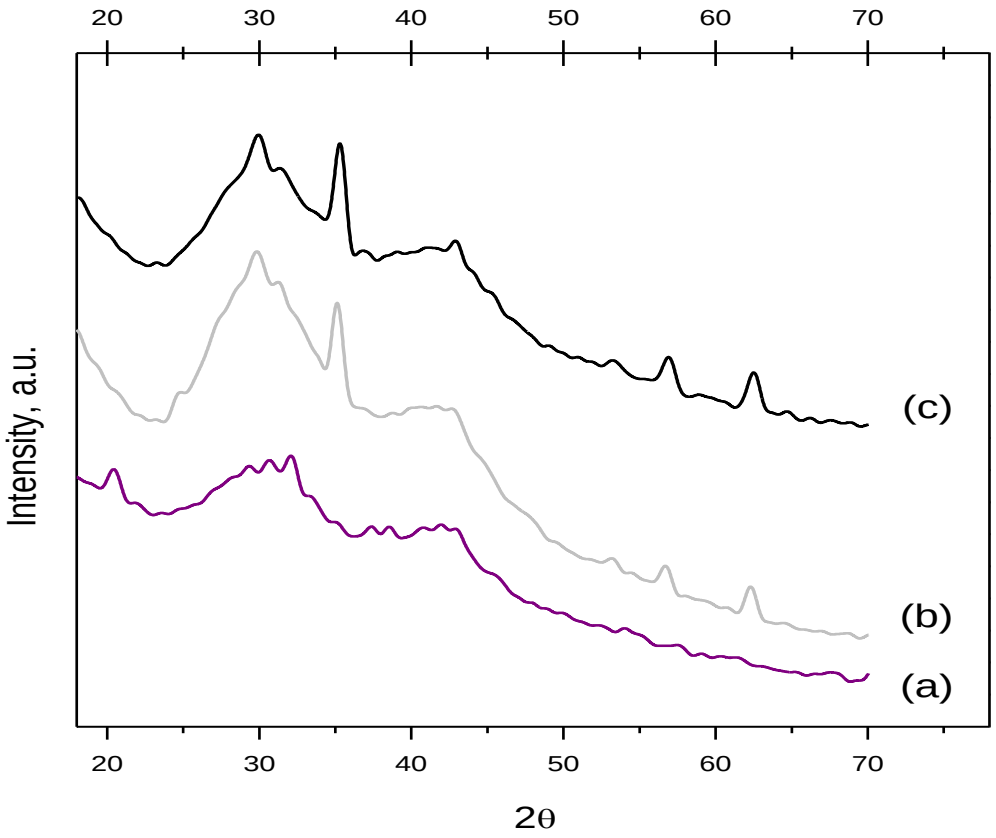

Figure 6. X-ray diffraction patterns obtained for **MWCNT-CMC-p** (a) before and after further thermal treatment at (b) 550 °C and (c) 900 °C under argon.

The presence of iron was confirmed by XPS analyses (Figure 7 and Table 2). From **MWCNT-CMC-p** to **MWCNT-CMC-p-900**, the atomic ratio Fe/C decreased from 0.385 to 0.024 (Table 2). Ion etching was performed on **MWCNT-CMC-p-900** at different durations, from 10 to 280 s (Figure 7c). Interestingly, iron content detected in the sample increased proportionally to ion etching duration; up to an atomic ratio Fe/C of 0.016 still lower than the one obtained for **MWCNT-CMC-p** before thermal treatment (Table 2). At this stage it has to be reminded that XPS gives the relative chemical composition of surfaces; depth 1–10 nm. Consequently, as mentioned earlier, one may assume that iron oxide nanoparticles got embedded within the carbonaceous framework, which is consistent with the fact that, before pyrolysis, iron salt was still homogeneously dispersed throughout the organic scaffold. This feature could be of great interest with a view to applications,. In particular, if employed such as anode material for lithium ion battery, the carbonaceous coating could both increase electronic conductivity and avoid pulverization during charge/discharge processes due to volume changes.[33] The carbonaceous coating could also act as a barrier to aggregation.

Further information was also obtained concerning the nature of the chemical bonds of iron. As for the Fe2p spectrum obtained for **MWCNT-CMC-p**, two main contributions centered at 711.4 eV and 724.5 eV, related to Fe2p3/2 and Fe2p1/2, respectively, were observed (Figure 7a), supporting the presence of iron (III) species most probably from iron (III) salts, $FeCl_3$, used in the pre-polymer mixture. This feature was also supported by the atomic ratio Cl/Fe of 0.269 (Table 2) and by the Cl2p spectrum showing a main contribution at 198.5 eV, associated with iron-chlorine bonds (see ESI for details). A weaker contribution centered at 709.4 eV suggested the presence of iron (II) species (Figure 7a and Table 2). After pyrolysis at 550 °C, the contribution at 709.4 eV slightly intensified, supporting the formation of magnetite Fe_3O_4, which contains both Fe^{2+} and Fe^{3+} cations in 1:2 ratio. This feature was also confirmed by O1s spectra with a strong contribution at 530.3 eV related to iron-oxygen bonds (see ESI for details). However, the Fe(II)/Fe(III) ratio as determined by XPS was 1:4 (Table 2), suggesting coexistence of both magnetite Fe_3O_4 and maghemite γ-Fe_2O_3 crystalline phases in 1:1 ratio. As for **MWCNT-CMC-p-900**, it has to be noticed that iron could not be detected without ion etching, which caused significant shifts of the Fe2p peaks due to reduction into metallic iron.

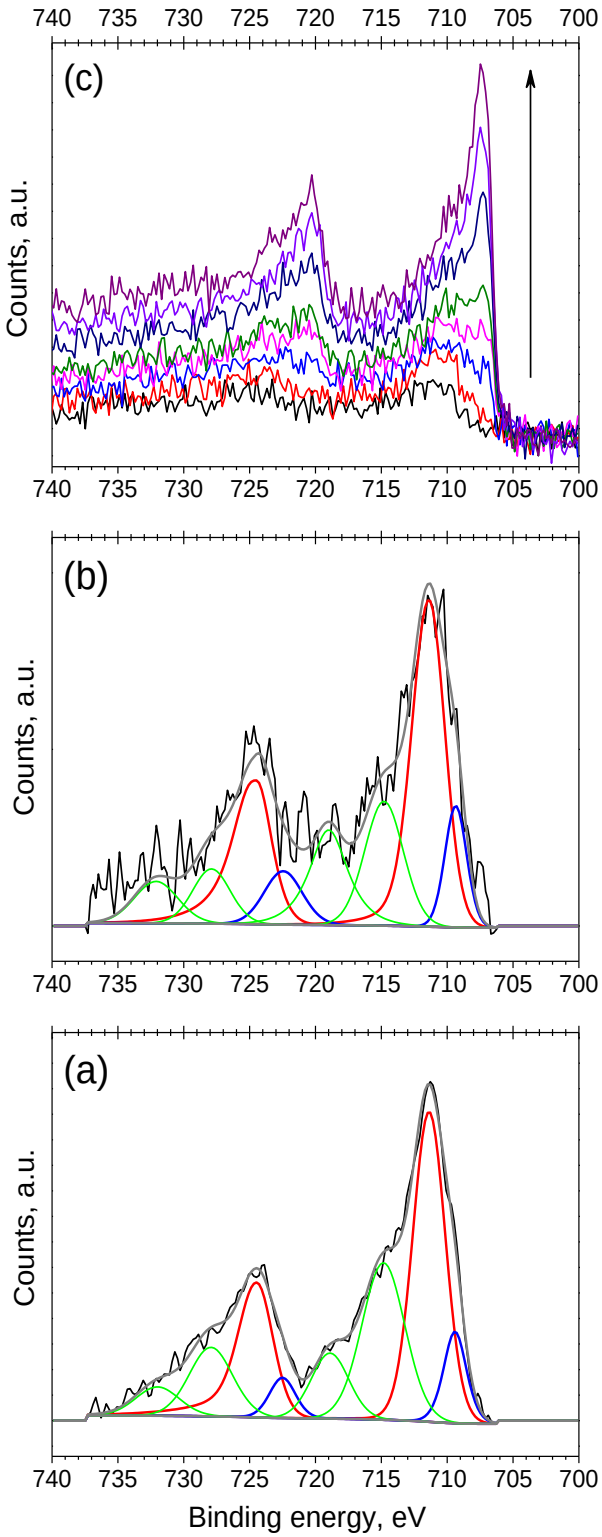

Figure 7. Fe2p X-ray photoelectron spectroscopy band-like spectra (black solid lines) and deconvoluted curves (colored solid lines) obtained for (a) **MWCNT-CMC-p** and (b) **MWCNT-CMC-p-550**. (c) Fe2p XPS band-like spectra obtained for **MWCNT-CMC-p-900**

and recorded after different ion etching durations: 0, 10, 40, 70, 100, 160, 220 and 280 s. The arrow shows the rise of Fe2p signal by increasing ion etching duration.

Table 1. [a]X-ray photoelectron spectroscopy and nitrogen sorption data obtained for **MWCNT-CMC-p** series. [b]The value in brackets was obtained after 280 s ion etching. [c]Area ratio of the contributions Fe(II) centered at 709.4 eV and Fe(III) centered at 711.4 eV obtained after deconvolution. Values obtained using [d]BET and [e]t-plot methods.

Nomenclature	Atomic ratios[a]				SA_{BET}[d]	SA_{micro}[e]	V_{Total}
	O/C	Fe/C	Cl/Fe	Fe(II)/Fe(III)[c]	$m^2.g^{-1}$	$m^2.g^{-1}$	$cm^3.g^{-1}$
MWCNT-CMC-p	0.385	0.034	2.689	0.21	/	/	/
MWCNT-CMC-p-550	0.092	0.005	0.477	0.24	920	914	0.33
MWCNT-CMC-p-900	0.024	0 (0.016)[b]	/	/	738	692	0.26

Beyond the formation of iron oxide nanoparticles, responsible for promising magnetic behaviors, pyrolysis allowed to increase both electrical conductivity (see ESI for electrochemical impedance spectroscopy data, Table S1) and porosity (Figure 8 and Table 2). As shown in Figure 8a, the nitrogen physisorption curve of **MWCNT-CMC-p-550** depicts a type I isotherm, typical of mainly microporous adsorbents. This sample displays significant BET surface area and pore volume as high as 920 $m^2.g^{-1}$ and 0.33 $cm^3.g^{-1}$ respectively. After pyrolysis at higher temperature, a soft hysteresis loop of type H4 could be observed (Figure 8b), typical of micro-mesoporous carbons.[34]

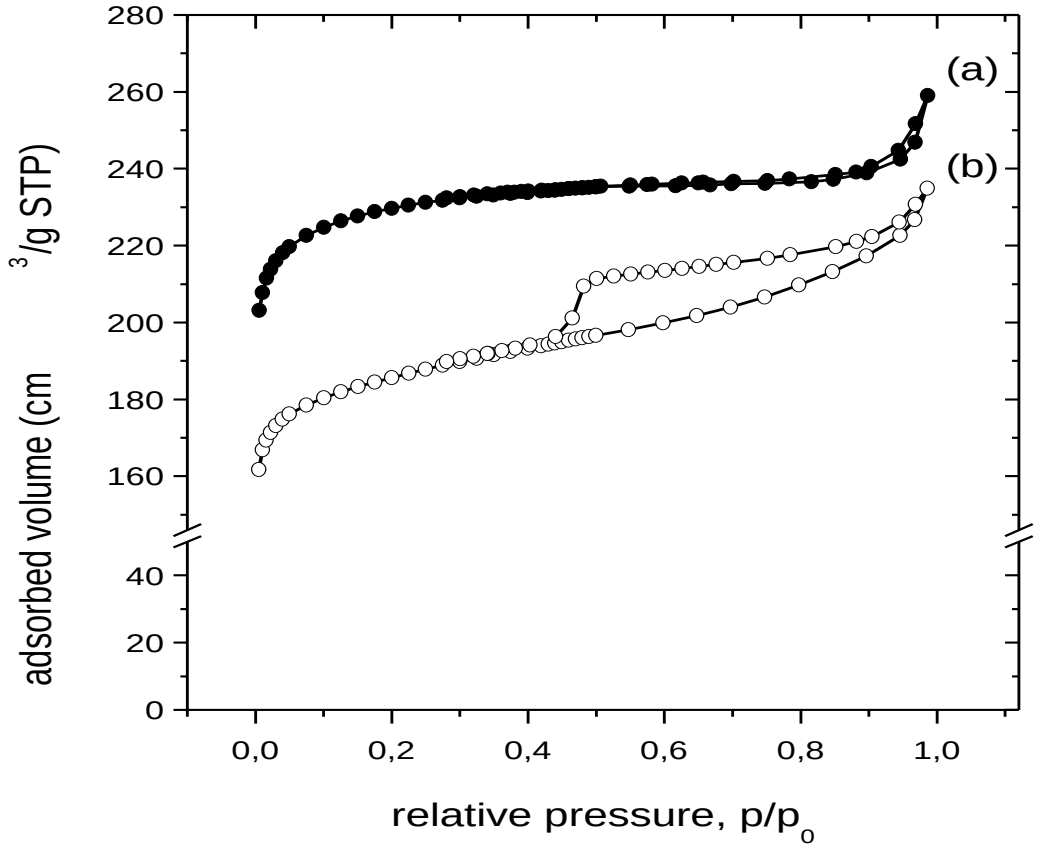

Figure 8. Nitrogen sorption isotherms obtained for (a) **MWCNT-CMC-p-550** and (b) **MWCNT-CMC-p-900**.

Conclusion

In this paper, we report the use of MWCNT-polysaccharide composites to stabilize Pickering emulsions. These stable emulsions were employed as soft templates for the design of materials with porous hierarchy. Actually, polymerization confined within the continuous aqueous phase allowed preparing. After pyrolysis, highly microporous and electrically conductive (see ESI for details) micrometric capsules could be obtained. Interestingly, iron oxide nanoparticles were also produced within the carbonaceous frameworks, due to the use of iron chloride in the pre-polymer mixture. The presence of such nanoparticles made our capsules magnetic. Combining pore hierarchy and magnetic properties with the well-known ability of carbonaceous materials as adsorbing and/or catalyst supports could be of interest for applications in catalysis and separation. Finally, the emulsion-templated approach allowed for confining the design of hierarchical porous structures at oil/water interfaces, which could

deserve also investigations as component of electrode materials in energy storage and conversion devices.

Authors information

Corresponding Authors

*E-mail: nicolas.brun@enscm.fr; Fax: +33 (0)4 67 14 38 52; Tel: +33 (0)4 67 14 48 24

*E-mail: andre.vioux@univ-montp2.fr; Fax: +33 (0)4 67 14 38 52; Tel: +33 (0)4 67 14 39 70

Notes

The authors declare no competing financial interest.

Acknowledgments

This work was conducted within the framework of ANR-10-LABX-05-01 "LABEX CheMISyst" program. Especially, Dr C.A. is grateful to "LABEX CheMISyst" for financial support. The authors would like to thank Franck Godiard and Didier Cot for electron microscopy and Thomas Cacciaguerra for XRD experiments. Drs O.F. and N.B. are grateful to François Fajula for its support and investment, especially regarding SECM.

References

1. B.-L. Su, C. Sanchez and X.-Y. Yang, *Hierarchically Structured Porous Materials*, Wiley-VCH, Weinheim, 2012.
2. C. Sanchez, H. Arribart and M. M. G. Guille, *Nature Materials*, 2005, **4**, 277-288.
3. R. Backov, *Soft Matter*, 2006, **2**, 452-464.
4. N. Brun, S. Ungureanu, H. Deleuze and R. Backov, *Chemical Society Reviews*, 2011, **40**, 771-788.
5. K. Valle, P. Belleville, F. Pereira and C. Sanchez, *Nature Materials*, 2006, **5**, 107-111.
6. S. Kubo, R. J. White, K. Tauer and M. M. Titirici, *Chemistry of Materials*, 2013, **25**, 4781-4790.
7. S. U. Pickering, *Journal of the Chemical Society*, 1907, **91**, 2001-2021.
8. B. P. Binks, *Current Opinion in Colloid & Interface Science*, 2002, **7**, 21-41.
9. F. Leal-Calderon and V. Schmitt, *Current Opinion in Colloid & Interface Science*, 2008, **13**, 217-227.
10. S. Arditty, V. Schmitt, J. Giermanska-Kahn and F. Leal-Calderon, *Journal of Colloid and Interface Science*, 2004, **275**, 659-664.
11. M. Destribats, B. Faure, M. Birot, O. Babot, V. Schmitt and R. Backov, *Advanced Functional Materials*, 2012, **22**, 2642-2654.
12. Y. Yang, Z. J. Wei, C. Y. Wang and Z. Tong, *Chemical Communications*, 2013, **49**, 7144-7146.

13. S. Lam, K. P. Velikov and O. D. Velev, *Current Opinion in Colloid & Interface Science*, 2014, **19**, 490-500.
14. S. Tasset, B. Cathala, H. Bizot and I. Capron, *Rsc Advances*, 2014, **4**, 893-898.
15. M. Depardieu, M. Nollet, M. Destribats, V. Schmitt and R. Backov, *Particle & Particle Systems Characterization*, 2013, **30**, 185-192.
16. M. Nollet, M. Depardieu, M. Destribats, R. Backov and V. Schmitt, *Particle & Particle Systems Characterization*, 2013, **30**, 62-66.
17. X. J. Chen, P. K. Eggers, A. D. Slattery, S. G. Ogden and C. L. Raston, *Journal of Colloid and Interface Science*, 2014, **430**, 174-177.
18. H. X. Yi, H. H. Song and X. H. Chen, *Langmuir*, 2007, **23**, 3199-3204.
19. W. Chen, X. Liu, Y. Liu and H. I. Kim, *Materials Letters*, 2010, **64**, 2589-2592.
20. Y. R. Li, J. Chen, L. Huang, C. Li, J. D. Hong and G. Q. Shi, *Advanced Materials*, 2014, **26**, 4789-+.
21. O. V. Kharissova, B. I. Kharisov and E. G. D. Ortiz, *Rsc Advances*, 2013, **3**, 24812-24852.
22. P. Bilalis, D. Katsigiannopoulos, A. Avgeropoulos and G. Sakellariou, *Rsc Advances*, 2014, **4**, 2911-2934.
23. M. G. Adsul, D. A. Rey and D. V. Gokhale, *Journal of Materials Chemistry*, 2011, **21**, 2054-2056.
24. T. Takahashi, K. Tsunoda, H. Yajima and T. Ishii, *Japanese Journal of Applied Physics Part 1-Regular Papers Brief Communications & Review Papers*, 2004, **43**, 3636-3639.
25. N. Minami, Y. J. Kim, K. Miyashita, S. Kazaoui and B. Nalini, *Applied Physics Letters*, 2006, **88**.
26. O. K. Kim, J. T. Je, J. W. Baldwin, S. Kooi, P. E. Pehrsson and L. J. Buckley, *Journal of the American Chemical Society*, 2003, **125**, 4426-4427.
27. N. B. C. Avendano, O. Fontaine, M. In, A. Mehdi, A. Stocco and A. Vioux, *Langmuir*, 2016, under revision.
28. N. Brun, L. Edembe, S. Gounel, N. Mano and M. M. Titirici, *ChemSusChem*, 2013, **6**, 701-710.
29. N. Brun, B. Julian-Lopez, P. Hesemann, G. Laurent, H. Deleuze, C. Sanchez, M. F. Achard and R. Backov, *Chemistry of Materials*, 2008, **20**, 7117-7129.
30. S. M. Saad, S. M. Sayyah, N. E. Metwally and A. A. Mourad, *Acta Polymerica*, 1988, **39**, 568-574.
31. L. S. Zhong, J. S. Hu, H. P. Liang, A. M. Cao, W. G. Song and L. J. Wan, *Advanced Materials*, 2006, **18**, 2426-+.
32. J. Jin, W. A. Hines, C. H. Kuo, D. M. Perry, A. S. Poyraz, Y. Xia, T. Zaidi, M. P. Nieh and S. L. Suib, *Dalton Transactions*, 2015, **44**, 11943-11953.
33. L. Zhao, M. M. Gao, W. B. Yue, Y. Jiang, Y. Wang, Y. Ren and F. Q. Hu, *Acs Applied Materials & Interfaces*, 2015, **7**, 9709-9715.
34. M. Thommes, K. Kaneko, A. V. Neimark, J. P. Olivier, F. Rodriguez-Reinoso, J. Rouquerol and K. S. W. Sing, *Pure and Applied Chemistry*, 2015, **87**, 1051-1069.

Graphical Abstract

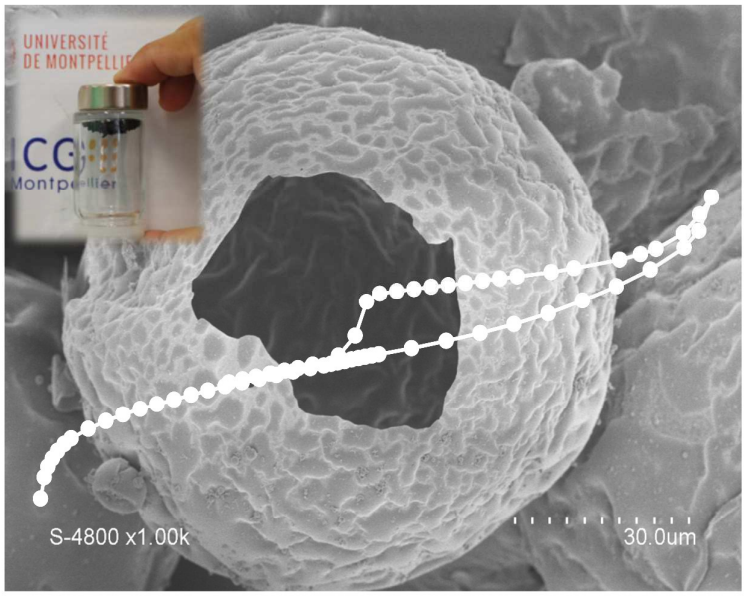

Templating polycondensation of furfural and phloroglucinol by O/W emulsions stabilized by CNT-carboxymethylcellulose composite particles allowed preparing conductive and magnetic microcapsules.